

Bionic Robot Motion Control Based on Visual Track and Gesture Measurement Glove Oriented to Rotation-Traction Manipulation Training

Haiyu He¹, Zhen Chen¹, Wenliang Lin^{*2}, Liguozhu³, Minshan Feng³, Liwei Shao⁴

¹Beijing Institute of Technology, Beijing China

²Capital Aerospace Machinery Co., Ltd., Beijing China

³Wangjing Hospital, Chinese Academy of Traditional Chinese Medicine, Beijing China

⁴Research Institute of BIT in Zhongshan, Guangdong China

* corresponding author E-mail: linwl010@126.com

Abstract: Rotation-Traction Manipulation (RTM) has been proved that is an effective treatment for cervical spondylosis. However, the manipulation is hard to grasp for beginners. In previous study, A prototype training robot has been proposed and obtained good training effect. During the manipulation process, we find that patients need to follow the doctor's hand gesture. In order to achieve better training experience. An algorithm based on computer vision and gesture measurement glove are proposed to simulate patients tracking hand trajectory in this paper. Firstly, the platform of RTM training robot is simply described. Then, a visual tracking and gesture measurement system are introduced to track the clinicians' gesture in the first step of manipulation. An improved Camshift algorithm is proposed to enhance the robustness of the tracking trajectory. Meanwhile, a gesture measurement glove is adopted to guaranteed the real-time performance and accuracy of gesture recognition. In this paper, experiments of visual track and gesture measurement carried out. The results show that the robot can track gestures well and satisfy the clinical application requirement.

Keywords: Visual track, Training robot, Rotation-Traction manipulation, Gesture measurement.

1. INTRODUCTION

More and more people suffer from cervical spondylosis due to bad living habits and work pressure[1]. At present, there is no widely approved radical cure for cervical spondylosis[2]. Conservative treatment is a widely adopted treatment. Among them, the rotation-traction manipulation of traditional Chinese medicine is widely used because of its significant efficacy and simple manipulation[3].

* This work is supported by Intelligent Equipment and The Technology of Automation Research and Development Platform under Grant 2016F2FC007.

The rotation-traction manipulation is mainly divided into two steps. In the first step, the patient follows the clinician's gesture and turns his head to reach the physiological limit of the cervical spine. In the second step, the clinician uses forearm to hold up the patient's mandible tightly, pulling up patient's head laxly in order to drag the locked vertebrae out of its capsule. Patient's neck is fragile, therefore, the manipulation must be performed by an experienced clinician [4].

The traditional pedagogy of rotation-traction manipulation is inefficient. Interns cannot obtain the patient's approval, so they have no chance to practice. It is crucial to develop a clinical teaching robot for RTM.

Benefitting from the development of technologies such as medical technology, robotics, computer science, mathematics, biomechanics, and biomedical engineering, robots are utilized in medical fields increasingly[5][6][7][8], including diagnosis, surgical, rehabilitation, medical services and other fields. Clinical teaching robot belongs to medical service robot, which mainly works for doctors and provides students with repeatable clinical platform to practice.

In previous studies [9][10], researchers have proposed a bionic robot which tracks doctor's hand based on visual tracking and visual servo. However, the gesture control of the clinician during the manipulation cannot be simulated, and the start or end of tracking still depends on remote controller, which is not enough.

A bionic robot based on visual track and gesture measurement glove control which is oriented to training the manipulation is proposed. The paper is organized as follows. Firstly, the platform of RTM training robot is simply described. Secondly, a visual tracking and gesture measurement system are introduced to track the clinicians' gesture in the first step of manipulation. Finally, experiments of visual track and gesture measurement were carried out.

2. PROTOTYPE OF TRAINING ROBOT

In previous studies [9][10], A two-degree-of-freedom rotating mechanism is designed to simulate the movement of the neck. An industrial camera is attached to the rotating

mechanism to capture images. The horizontal mechanical joint position is limited to 75 degrees, and the vertical mechanical position limitation is 30 degrees. The two-degree-of-freedom rotating mechanism is connected to a variable stiffness structure, and an electromagnet is attached to its end-effector to mimic the process of the human cervical spine detaching from the joint capsule. The mechanical structure is shown in the Fig.1.

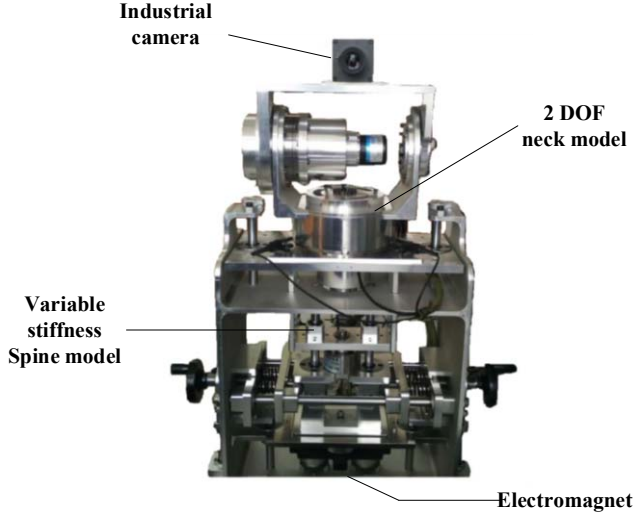


Fig.1. The prototype

3. GESTURE MEASUREMENT GLOVES

The real time gesture measurement glove was adopted to simulate physician's gesture command during the first step of the manipulation. The gesture of clinician was utilized as the basis for tracking. The structure of gesture measurement glove is shown as Fig.2.

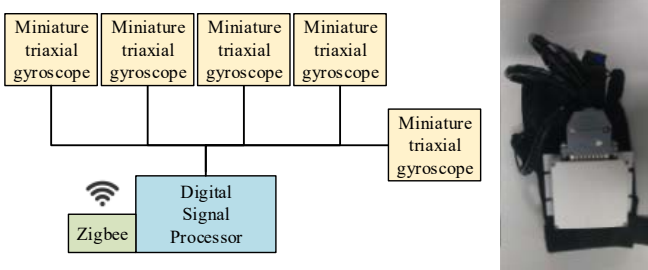


Fig.2. gesture measurement glove architecture

Triaxial miniature gyroscopes were placed on every fingertip. Gyroscopes data were gathered by DSP and wirelessly transmitted to the computer through Zigbee. The estimation of finger gesture is the core of the measurement glove. In this paper, the Kalman filter algorithm is utilized to estimate the finger gesture [11].

Assume that the system's prior estimates are

$$\bar{x}_k = Fx_{k-1} + Bu_{k-1}. \quad (1)$$

The F is state matrix, B represents input matrix. Define observed value is

$$z_k = H_k x_k + v_k. \quad (2)$$

Where H_k , v_k , x_k denoting the observation matrix, measurement error and optimal estimate of the system at time k respectively. The prior estimate of the covariance matrix P_k at time k can be obtained from the value at time $k-1$:

$$\bar{P}_k = F P_{k-1} F^T + Q_{k-1}. \quad (3)$$

Where Q represents the noise covariance matrix, and thus the Kalman gain matrix is:

$$K_k = \bar{P}_k H_k^T (H_k \bar{P}_k H_k^T + R_k)^{-1}. \quad (4)$$

From this, the optimal estimates of x_k and P_k at time k are obtained:

$$x_k = \bar{x}_k + K_k (z_k - H_k \bar{x}_k), \quad (5)$$

$$P_k = (I - K_k H_k) \bar{P}_k. \quad (6)$$

In this paper,

$$x = [\alpha \quad q_{bias}]^T, \quad (7)$$

$$F = \begin{bmatrix} 1 & -dt \\ 0 & 1 \end{bmatrix}, \quad (8)$$

$$B = [dt \quad 0]^T, \quad (9)$$

$$u = Gyro, \quad (10)$$

$$H = [1 \quad 0], \quad (11)$$

The α , q_{bias} and Gyro represent the optimal estimate of finger gesture, gyro zero offset and the measured value of the gyroscope, dt is the filter sampling time.

The relationship between Gyro and finger gesture α of one finger was shown in Fig.3.

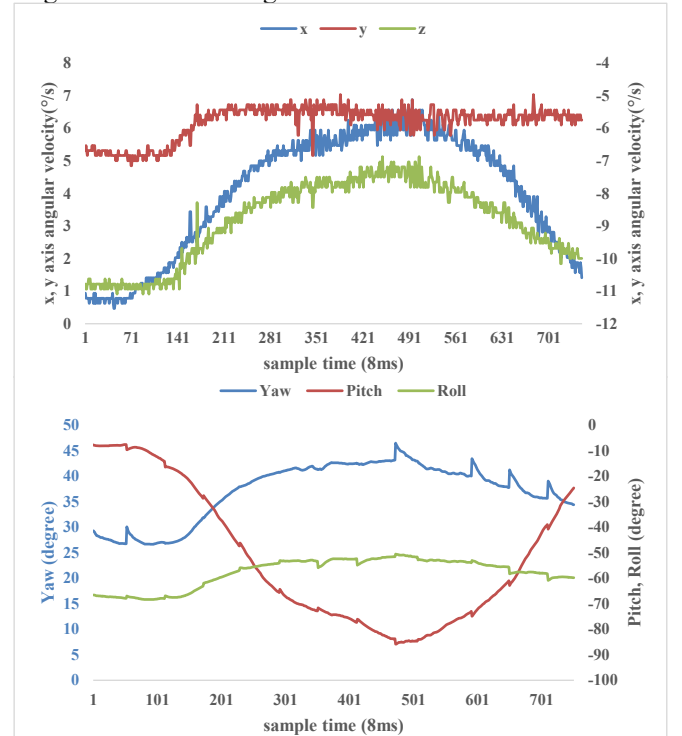


Fig.3. The relationship between Gyro and finger gesture of one finger.

4. HAND TRACKING AND ROBOT CONTROL

To accomplish hand tracking task, a tracking algorithm was utilized in this paper.

4.1. The tracking algorithm

The tracking algorithm should satisfy the need for real time, and the hand should be tracked well. Camshift is a conventional algorithm [12][13]. The main steps of the conventional algorithm are shown as follows:

Steps 1: the target area should be selected manually;

Steps 2: the histogram of the target would be modeled. And the back projection would be calculated based on the histogram.

Step 3: the search window size and the target center are calculated as follows:

$$M_{00} = \sum p(x, y), \quad (12)$$

$$M_{10} = \sum xp(x, y), \quad (13)$$

$$M_{01} = \sum yp(x, y). \quad (14)$$

Hence the center (x_c, y_c) is:

$$x_c = \frac{M_{10}}{M_{00}}, \quad (15)$$

$$y_c = \frac{M_{01}}{M_{00}}. \quad (16)$$

Set the search window is a circle, and the adaptive radius is:

$$R_s = 2\sqrt{M_{00} / 256}; \quad (17)$$

Step 4: calculate the shape of the target area:

$$M_{11} = \sum_x \sum_y xyp(x, y), \quad (18)$$

$$M_{20} = \sum_x \sum_y x^2 p(x, y), \quad (19)$$

$$M_{02} = \sum_x \sum_y y^2 p(x, y). \quad (20)$$

Define:

$$a = \frac{M_{20}}{M_{00}} - x_c^2, \quad (21)$$

$$b = 2\left(\frac{M_{11}}{M_{00}} - x_c y_c\right), \quad (22)$$

$$c = \frac{M_{02}}{M_{00}} - y_c^2. \quad (23)$$

So, the length L, the width W, the angle θ of the area are calculated as below:

$$L = \sqrt{\frac{a+c + \sqrt{b^2 + (a-c)^2}}{2}}, \quad (24)$$

$$W = \sqrt{\frac{a+c - \sqrt{b^2 + (a-c)^2}}{2}}, \quad (25)$$

$$\theta = \frac{1}{2} \arctan\left(\frac{b}{a-c}\right). \quad (26)$$

An improved Camshift was utilized in this paper. Firstly, model the histogram of the target h_o and the histogram of the whole image h_w . Then define the background histogram h_b .

Obviously, the histogram of the whole picture can be divided into the arithmetic sum of the target histogram and the background histogram,

$$h_w = h_o + h_b. \quad (27)$$

In order to obtain a more accurate target area, a back-projection operation was performed on the whole image, and the target connected domain in the probability map was regarded as an optimal estimation of the tracking target.

Hence an optimal estimation \bar{h}_o of target histogram was obtained, and a new background histogram

$$\bar{h}_b = h_w - \bar{h}_o. \quad (28)$$

During target tracking, similar features in the background histogram will interfere with the target. In order to reduce the impact of these features, the weight of these features in the target histogram needs to be reduced.

Define the criterion:

$$\delta_u = \frac{\bar{h}_o + \bar{h}_o - \bar{h}_b}{\max(\bar{h}_o)}. \quad (29)$$

The feature will be rescaled depends on the result of δ_u and the optimized target histogram was obtained.

Finally normalize the hop according to the following equation:

$$\hat{h}_{op} = \frac{h_{op}}{\text{Max}(h_{op})} \times 255 \quad (30)$$

The steps of the improved Camshift are shown as follows:

Steps 1: the same as the conventional Camshift;

Steps 2: the different feature histogram would be modeled according to (27)-(30), and the back projection is calculated by using the optimized target histogram;

Steps 3, 4: the same as the conventional Camshift;

Steps 5: set

$$T = (L + W) / 2. \quad (31)$$

And a new search window is defined

$$x \in (x_c - T, x_c + T), \quad (32)$$

$$y \in (y_c - T, y_c + T). \quad (33)$$

In the new search window, $x_c, y_c, R_s, L, W, \theta$ in steps 3, 4 would be recalculated.

This method also can be utilized in other color spaces such as YCrCb in which the skin can be recognized easily [14].

The comparison between the conventional Camshift (left) and the improved Camshift (right) is shown in Fig.4 and Fig.5 The estimated location of target is marked in pictures. The target in Fig.4 is the white ball and the target in Fig.5 is the right clenched hand.



Fig.4. The tracking result of the blue book

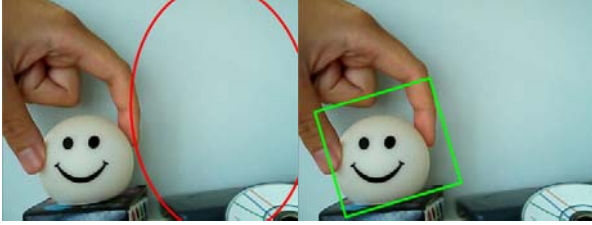


Fig.5. The tracking result of the white ball

4.2. Image position control

After tracking, the hand position would be transformed into the robot position command as the input of robot position control loop, the control system is shown in Fig.6 To accomplish this, a robot-image control algorithm was utilized in this paper.

Define the image space as the state space of the hand. The state space was split into five regions shown in Fig.7. A two-dimensional state vector was utilized to represent the state of the hand,

$$\mathbf{x} = (u, v)^T. \quad (34)$$

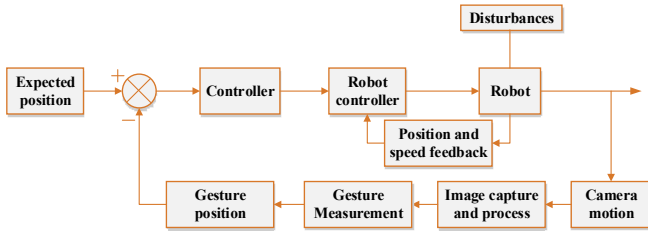


Fig.6. The hand position control system

In the state space, Ω_0 is defined as the stable state.

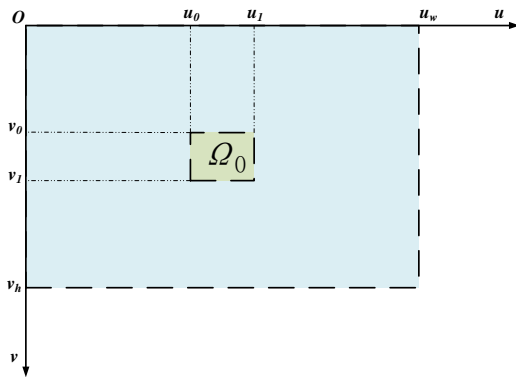


Fig.7. The state space of the hand

Based on the state space, the position error was defined as

$$\mathbf{e} = \mathbf{R}\mathbf{c} - \mathbf{x}, \quad (35)$$

where \mathbf{R} is a 2×4 matrix and \mathbf{c} are a four dimensional column vector $(u_0, u_1, v_0, v_1)^T$. The value of \mathbf{R} depends on the x region.

$$\mathbf{e} = \begin{bmatrix} a & b & 0 & 0 \\ 0 & 0 & c & d \end{bmatrix} \begin{bmatrix} u_0 \\ u_1 \\ v_0 \\ v_1 \end{bmatrix} - \begin{bmatrix} 1 & 0 \\ 0 & 1 \end{bmatrix} \begin{bmatrix} u \\ v \end{bmatrix}, \quad (36)$$

$$a = \begin{cases} 1 & \text{if } (u_0 - u) \geq 0 \\ 0 & \text{else} \end{cases}$$

$$b = \begin{cases} 1 & \text{if } (u_1 - u) \leq 0 \\ 0 & \text{else} \end{cases}$$

$$c = \begin{cases} 1 & \text{if } (v_0 - v) \geq 0 \\ 0 & \text{else} \end{cases}$$

$$d = \begin{cases} 1 & \text{if } (v_1 - v) \leq 0 \\ 0 & \text{else} \end{cases} \quad (37)$$

So the position command was given by

$$\mathbf{u}_t = \mathbf{k}\mathbf{e}, \quad (38)$$

$$\mathbf{k} = \begin{bmatrix} \eta_u & 0 \\ 0 & \eta_v \end{bmatrix}. \quad (39)$$

The motor driver utilized in this paper only have one interface of position command, for convenience, the motor was treated as a step motor, so the position command was partitioned into

$$\mathbf{u}_t = \begin{bmatrix} \eta_u & 0 \\ 0 & \eta_v \end{bmatrix} \begin{bmatrix} \text{sign}(e_u) \\ \text{sign}(e_v) \end{bmatrix} = \begin{bmatrix} \eta_u \text{sign}(e_u) \\ \eta_v \text{sign}(e_v) \end{bmatrix}. \quad (40)$$

Though a robust tracking algorithm was utilized, there still exist some errors. Such as the object occlusion problem. To protect the robot, the density of object points was evaluated. According to the improved Camshift algorithm, the new M_{00} , L , W calculated in step 5 were introduced,

$$\text{density} = \frac{M_{00}}{128\pi LW}. \quad (41)$$

The density will be compared with a given threshold as the criteria of tracking success.

4. EXPERIMENT

An experiment prototype was developed. In this paper, the industrial camera JHSM36f with the resolution 752×480 was attached to joint 1.

Before gesture tracking, the robot is in standby mode and waiting for hand gesture signals.

Operators wear gesture measuring gloves and make prescribed gestures. The robot judges whether the gesture meets the tracking requirements, and when the difference between the gestures of the thumb and the index finger is greater than a given threshold, visual tracking starts.

The hand would move around the stable region with a fixed gesture, hence the state errors e_x , e_y approach to sine curves, the speed command w_x , w_y will be evaluated. The gesture measurement results and visual tracking results are shown in Fig.8-Fig.10.

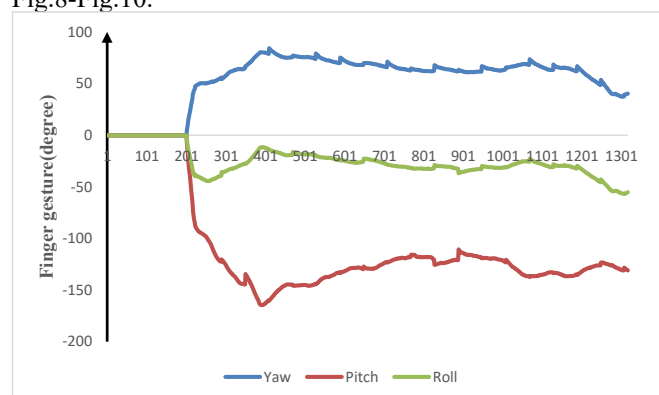


Fig.8. Thumb gesture

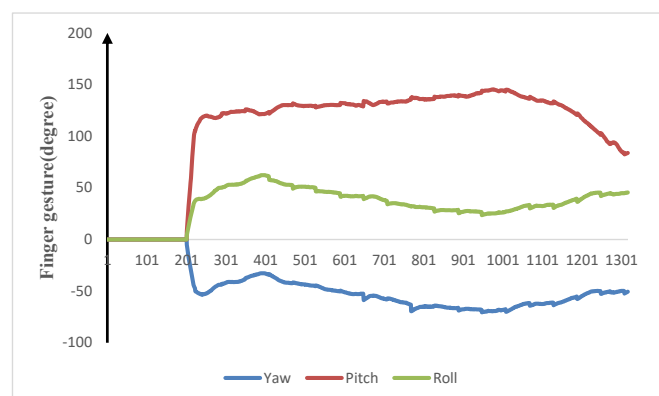


Fig.9. Forefinger gesture

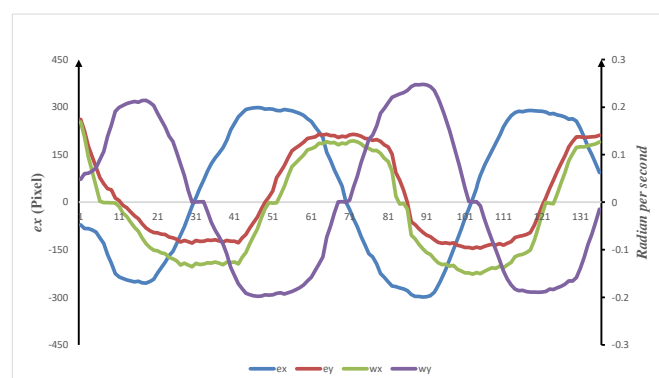


Fig.10. e_x , e_y and w_x , w_y

5. CONCLUSION

In this paper, an improved Camshift algorithm is proposed to track human hand based on RTM training robot. When hand's movement occurs, the algorithm is utilized to transform the position deviation into speed command and

allow the robot follow the doctors hand in real time. Meanwhile, a gesture measurement glove is designed to recognize clinician's gesture and control the robot. The experiment results suggest that the visual track and gesture control system satisfies the requirement of clinical application. The robot proposed in this article can more realistically simulate the interaction between patients and clinicians during manipulation, improve teaching efficiency, and provide a better user experience.

REFERENCES

- [1] Tzong-Hann Yang, Sudha Xirasagar, Yen-Fu Cheng, Chuan-Song Wu, Yi-Wei Kao, Ben-Chang Shia, Heng-Ching Lin. Association of cervical spondylosis with obstructive sleep apnea[J]. Sleep Medicine, 2020, 71.
- [2] DAI Yi-guang, LI Xiu-xia, MA Chun-jie. Clinical observation on the treatment of cervical spondylotic radiculopathy by bone-setting manipulation [J]. Chinese Manipulation and Rehabilitation Medicine, 2020, 11(13):14-16. (in Chinese)
- [3] XIE Guan-you, Zhang lin, XU miao, etc.. Analysis of objective evaluation of massage on cervical spondylopathy therapeutic effect [J]. Chinese Manipulation and Rehabilitation Medicine, 2020, 11(13):21-23. (in Chinese)
- [4] L. G. Zhu and Q. Zhang. Clinical observation on rotational-traction manipulation for treatment of the cervical spondylotic of the neuroradicular type, China Journal of Orthopedics and Traumatology, Vol. 18, No. 8, pp. 489-490, 2005. (in Chinese)
- [5] Ziqiang NI, Tianmiao WANG, Da LIU, "Survey on Medical Robotics," JOURNAL OF MECHANICAL ENGINEERING, vol. 51, pp. 45-52, July 2015.
- [6] WANG Tian-miao, LI Wei, LIU Da, LIU Jing-meng, etc. , "study of robot-assisted orthopedic oreratio," ROBOT, vol. 25, pp.255-258, May 2003.
- [7] GAO Huanbing, LU Shouyin, WANG Tao, etc., "Research and Development of Chinese Medical Massage Robot," ROBOT, vol. 33, pp. 553-562, September 2011.
- [8] Yu shunian, Ma lüzhong, Chen Exi, "Study on a Novel Series-parallel Chinese Massage Manipulator," CHINA MECHANICAL ENGINEERING, vol. 19, pp.1773-1778, 2005.
- [9] Y. Huang, L. Yao, M. Feng, L. Zhu and J. Li, "Design of cervical spine mechanical emulator for rotation-traction manipulation drills," 2014 IEEE 13th International Workshop on Advanced Motion Control (AMC), Yokohama, 2014, pp. 621-626
- [10] G. Li, P. Lu, L. Shao, C. Gao and J. Li, "The application of impedance control in rotation-traction manipulation bionic robot," 2017 36th Chinese Control Conference (CCC), Dalian, 2017, pp. 6810-6816
- [11] H. Ferdinando, H. Khoswanto and D. Purwanto, "Embedded Kalman Filter for Inertial Measurement Unit (IMU) on the ATmega8535," 2012 International Symposium on Innovations in Intelligent Systems and Applications, Trabzon, 2012, pp. 1-5
- [12] ZUO Jun-Yi, LIANG Yan, PAN Quan, ZHAO Chun-Hui, ZHANG Hong-Cai, "Camshift Tracker Based on Multiple Color Distribution Models," ACTA AUTOMATICA SINICA, vol. 34, July 2008, pp.736-742.
- [13] PENG Juanchun, GU Lizhong, SU Jianbo, "The Hand Tracking fOr HumanOld ROBot Using Camshift AlgOrithm and Kalman Filter," JOURNAL OF SHANGHAI JIAOTONG UNIVERSITY, vol. 40, July 2006, pp.1161-1165.
- [14] Douglas Chai, King N Ngan, "Automatic Face Location for Videophone Images," TENCON '96. Proceedings., 1996 IEEE TENCON, pp.137-140.
- [15] Zhengyou Zhang, "A Flexible New Technique for Camera Calibration," IEEE TRANSACTIONS ON PATTERN ANALYSIS AND MACHINE INTELLIGENCE, VOL. 22, November 2000, pp.1330-1334.